ORIGINAL PAPER

Partial stripping of Ag atoms from silver bilayer on a Au(111) surface accompanied with the reductive desorption of hexanethiol SAM

Toshihiro Kondo · Kazuhisa Tamura · Satoru Takakusagi · Ken Kitamura · Masamitu Takahasi · Jun'ichiro Mizuki · Kohei Uosaki

Abstract The interfacial structures of Ag bilayer prepared by underpotential deposition on Au(111) (Ag(2ML)/Au (111)) were determined by ex situ scanning tunneling microscopy and in situ surface X-ray scattering measurements before and after oxidative adsorption and after reductive desorption of a self-assembled monolayer (SAM) of hexanethiol (C_6SH) in alkaline ethanol solution. While no structural change was observed after oxidative formation of C_6SH SAM on the Ag(2ML)/Au(111) in an ethanol solution containing 20 mM KOH and 0.1 mM C_6SH, some of the Ag atoms in the bilayer were stripped when the SAM was reductively desorbed.

Keywords Au(111) · Ag underpotential deposition (UPD) · Self-assembled monolayer (SAM) · Surface X-ray scattering (SXS) · Scanning tunneling microscope (STM)

Dedicated to Professor J. O'M. Bockris on the occasion of his 85th birthday.

T. Kondo
Graduate School of Humanities and Sciences,
Ochanomizu University,
2-1-1, Ohtsuka, Bunkyo-ku,
Tokyo 112-8610, Japan

K. Tamura · M. Takahasi · J. Mizuki
Japan Atomic Energy Agency,
Koto, Sayo-cho,
Hyogo 679-5148, Japan

S. Takakusagi · K. Kitamura · K. Uosaki (✉)
Physical Chemistry Laboratory, Division of Chemistry,
Graduate School of Science, Hokkaido University,
Sapporo 060-0810, Japan
e-mail: uosaki@pcl.sci.hokudai.ac.jp
url: http://pchem.sci.hokudai.ac.jp

Introduction

Self-assembled monolayers (SAMs) of alkylthiols on gold have been extensively studied because of their wide range of applications including sensors and molecular electronic devices [1–8]. There are many structural studies on alkylthiol SAMs on gold, especially on Au(111), using scanning tunneling microscopy (STM) with molecular resolution [9–20]. STM observation of SAMs on Au(111) at high coverage revealed that there are many defects in SAMs such as missing rows and pits. The pits are vacancy islands of gold atoms, which are well known to be formed in the very early stage of the self-assembly process [14, 15]. It is, therefore, very important to know how the vacancy islands are formed for full understanding of the self-assembly mechanism. At least three possible mechanisms for vacancy island formation have been proposed: chemical etching of the gold surface by alkylthiols [10–12], compression of the surface lattice [20], and injection of more gold atoms than expected for the reconstruction lifting of the gold surface [9]. When alkylthiol SAMs are formed on a silver surface, atomic distance of which is very close to that of gold, similar pits with mono- and bi-atomic depths are also observed by STM, although pit size is slightly smaller than that on Au(111) [21–23]. On the other hand, only molecular defects without pits are observed when SAMs are formed on a Ag monolayer prepared by underpotential deposition (UPD) on Au(111) [24–26]. The origin of the pit formation is not clear yet and the information of not only the structural change of the substrate surface but also the loss of the substrate atom during the formation and desorption of the SAM is essential to clarify the origin of the pit.

Although STM and surface X-ray scattering (SXS) are very useful to investigate the interfacial structure with an atomic resolution in situ, they cannot detect the loss of the surface atoms during these processes as far as homogeneous substrates such as Au(111) and Ag(111) are used. Recently, we reported that a pseudomorphic Ag monolayer and bilayer were formed on a Au(111) surface by UPD at 50 mV (vs. Ag/Ag^+) and 10 mV, respectively [27]. We also found that although the structure of the Ag UPD monolayer changed in air, the Ag UPD bilayer was very stable even after exposure to air (Uosaki et al., in preparation). Thus, if we employ the Ag bilayer prepared by UPD on Au(111), Ag(2ML)/Au(111), as a substrate for the SAM formation/desorption, we should be able to detect the loss of Ag atoms during the formation and desorption of the SAM by SXS.

In this paper, the interfacial structures of Ag(2ML)/Au(111) before and after the oxidative adsorption and reductive desorption of a hexanethiol (C_6SH) SAM in an ethanol solution containing 20 mM KOH and 0.1 mM C_6SH were investigated by ex situ STM and in situ X-ray reflectivity measurement, one of the SXS methods. Although the surface structure did not change during oxidative formation of the SAM on the Ag(2ML)/Au(111), some of the Ag atoms in the bilayer were stripped when the SAM was reductively desorbed.

Experimental

A Au(111) substrate, which was prepared by vacuum evaporation of gold onto a fleshly cleaved mica sheet kept at 300 °C during evaporation, was used as a substrate for ex situ STM measurements. This provides the (111) oriented surface [14, 15, 17].

A Au(111) single crystal disk, which was purchased from the Surface Preparation Laboratory (The Netherlands), was used as a substrate for the SXS measurement after being treated as previously reported [28, 29].

Prior to each measurement, the Au(111) substrate was flame-annealed using a hydrogen flame and slowly cooled in air. It was then transferred to an electrochemical cell with the surface being covered with a drop of pure water to avoid any surface contamination [27, 29]. Ag bilayers on Au(111) were prepared by UPD in an electrolyte solution containing 50 mM H_2SO_4 (Wako Pure Chemicals) and 1 mM Ag_2SO_4 (Wako Pure Chemicals) at 10 mV (vs. Ag/Ag^+). A meniscus configuration was employed in the case of the Au(111) single crystal disk as previously reported [27]. After the Ag UPD, the electrodes (Ag(2ML)/Au(111)/mica for STM study and Ag(2ML)/Au(111) for SXS study) were washed with Milli-Q water (Yamato, WQ-500) and with ethanol (Wako Pure Chemicals).

For the ex situ STM study, C_6SH SAM was formed by dipping the Ag(2ML)/Au(111)/mica into an ethanol solution containing 50 μM C_6SH for 12 h and reductive desorption of the C_6SH SAM/Ag(2ML)/Au(111)/mica was carried out in a 10 mM KOH aqueous solution.

For the SXS study, the electrode (Ag(2ML)/Au(111)) was transferred to a spectroelectrochemical cell [30]. An ethanol solution containing 20 mM KOH and 0.1 mM C_6SH was introduced to the cell while keeping the potential at −1.4 V (vs. Ag/AgCl). The reflectivity measurement was carried out at this potential after the electrode surface was pushed to a 6.0 μm thick Mylar (Chemplex, D) window until the thickness of the solution layer between the electrode surface and the Mylar window was reduced to ca. 30 μm (thin layer configuration). The measurements were also carried out in thin layer configuration at 0 and −1.4 V after the potential was scanned to 0 V and then to −1.4 V with a scan rate of 20 mV s^{-1} with a thick layer configuration (electrolyte thickness: ca. 5 mm).

Results and discussion

Figure 1 shows ex situ STM image of the Ag(2ML)/Au(111) surface. Before the SAM formation, atomically flat surface with a step of mono-atomic height was observed as shown in Fig. 1a.

After the formation of the C_6SH SAM on the Ag(2ML)/Au(111) surface, atomically flat surface with several hollows was observed in the wide range image. Expanded image (Fig. 1b) shows that the depth of these hollows is ca. 0.1 nm, indicating that these hollows are not vacancy islands as the depth of the vacancy islands should be 0.24 nm. Schweizer and Kolb reported similar hollows for ethanethiol SAM formed on a Ag(111) surface [23]. Ordered bright spots were also observed in Fig. 1b. Spacing between these bright spots is 0.48±0.03 nm, which is slightly smaller than those (0.50 nm) generally observed for the alkylthiol SAMs on Au(111) and Ag(111) surfaces [9–23]. Many defects of SAM were observed and the number of the defects is much larger than those generally observed for alkylthiol SAMs on Au(111) and Ag(111) [9–23], suggesting that lateral molecular arrangement of the SAM is not completely matched with the atomic arrangement of the substrate.

Figure 1c shows ex situ STM image after the reductive desorption of the C_6SH SAM from the Ag(2ML)/Au(111) surface. The surface became very rough with mono- and bi-atomic height.

These results show that the substrate surface was roughened when the SAM was reductively desorbed, but the STM measurements cannot tell if the surface atoms were lost to the solution.
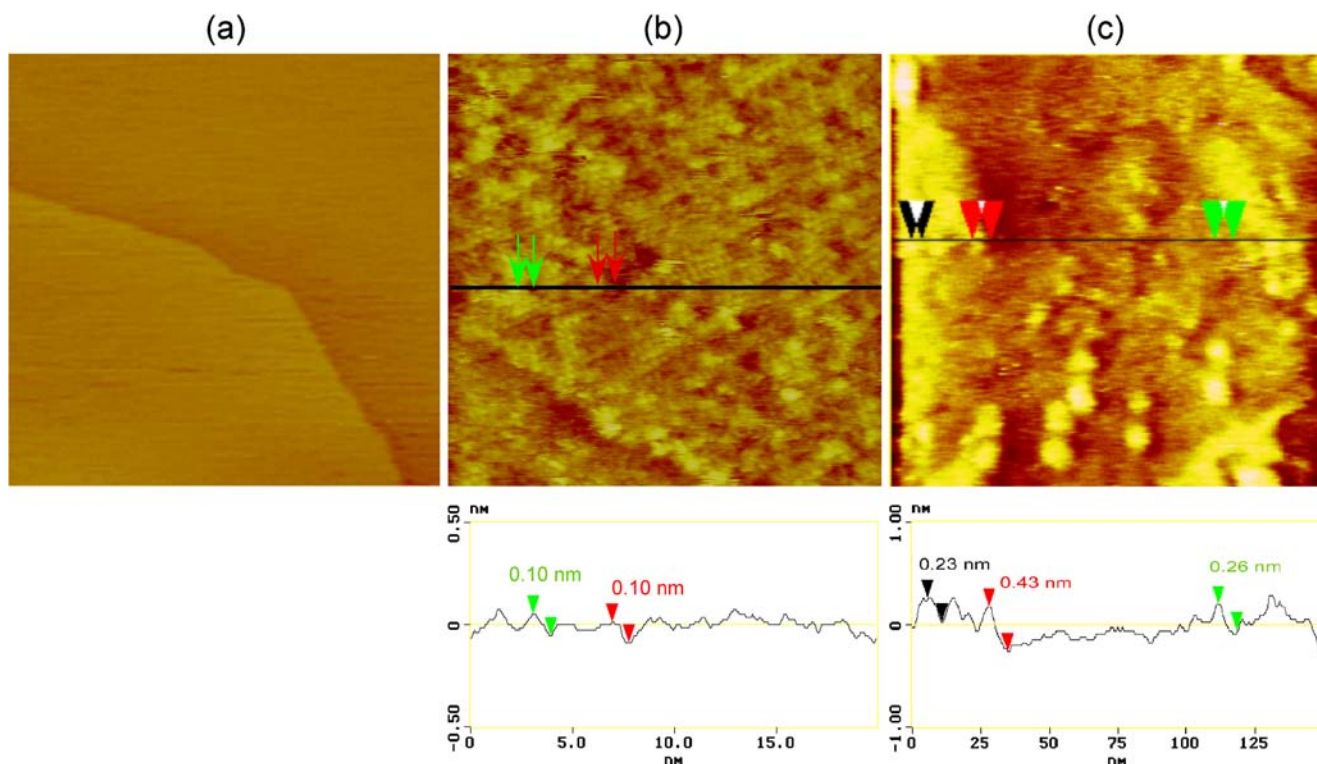
Fig. 1 **a** Ex situ STM image (100×100 nm^2) of the Ag(2ML)/Au (111) surface. $E_{tip}=50$ mV, $I_{tip}=350$ pA. **b** Ex situ STM image (20×20 nm^2) and cross-section of the Ag(2ML)/Au(111) surface after the C$_6$SH SAM formation. $E_{tip}=300$ mV, $I_{tip}=30$ pA. **c** Ex situ STM image (150×150 nm^2) and cross-section image after the reductive desorption of the C$_6$SH SAM on the Ag(2ML)/Au(111). $E_{tip}=50$ mV, $I_{tip}=600$ pA

In order to clarify this point, X-ray reflectivity measurements were carried out. Figure 2 shows reflectivity profiles of the Ag(2ML)/Au(111) electrode measured at (a) −1.4 V before the potential scan, (b) 0 V after the potential scan, and (c) −1.4 V after the potential cycle. Standard errors of the scattered X-ray reflectivity were shown as error bars in the figure. Structures along the direction normal to the electrode surface were quantitatively determined from the least square fitting to the reflectivity data with a kinematical

calculation based on a specific interfacial model [29, 31] consisting with three layers on top of the Au(111)-(1×1) substrate in both cases, i.e., Ag/Ag/Au on Au(111)-(1×1) at −1.4 V, where SAM is not on the surface, and S/Ag/Ag on Au(111)-(1×1) at 0 V, where SAM is on the surface. Thus, atomic form factors for the first, second, and third layers were of Au, Ag, and Ag at −1.4 V and of Ag, Ag, and S at 0 V. For the SAM layer, only the contribution of sulfur was considered in the fitting because the electron density of

Fig. 2 The reflectivity profiles of Ag(2ML)/Au(111) electrode measured in an ethanol solution containing 20 mM KOH and 0.1 mM C$_6$SH at **a** −1.4 V before the potential scan, **b** 0 V after the potential scan, and **c** −1.4 V after the potential cycle between −1.4 and 0 V. *Circles* and *solid lines* are experimental data and calculated curves fitted by the least squares method with kinematical calculation, respectively. Standard errors of the scattered X-ray intensity are shown as *error bars* in the figure
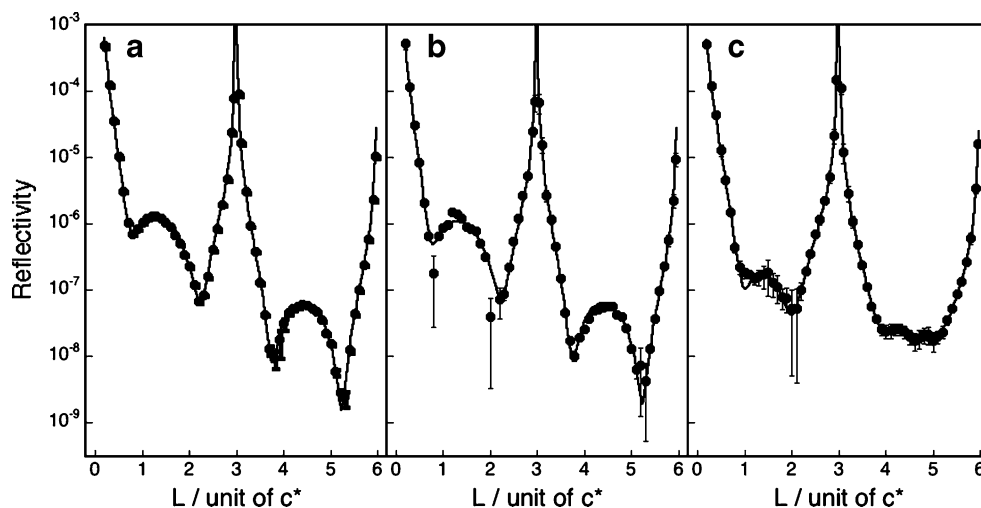
carbon atom is smaller than that of sulfur atom. The structural parameters obtained by the least square fitting of the experimental data with a kinematical calculation at these potentials are listed in Table 1.

At −1.4 V before the potential scan, where the C$_6$SH SAM cannot be formed [32–35], the best fit data showed that the Ag UPD bilayer perfectly remained on the Au (111)-(1×1) surface, showing that the Ag UPD bilayer on the Au(111) substrate is very stable, even after being transferred to the cell under air atmosphere and after dipping into the alkaline ethanol solution at −1.4 V.

The best fit data at 0 V after the anodic potential scan, where the C$_6$SH SAM is oxidatively formed [32–35], showed a sulfur layer with 1/3 coverage, which is in exact agreement with previous results [4, 21–23], on the Ag bilayer with coverages of 1 for both first and second Ag layers on the Au(111)-(1×1) surface, suggesting that no pits were present at the C$_6$SH SAM/Ag(2ML)/Au(111). Since the alkyl chain should also affect the structure parameters, although it was neglected in the fitting as it is expected to be small as described above, the distance between the second Ag and the S layers became larger than the reported values (ca. 2.6 Å) [26, 36, 37] and then the RMS value in the S layer became much larger.

The best fit data at −1.4 V, after the potential was scanned back from 0 to −1.4 V so that the C$_6$SH SAM should be reductively desorbed [32–35], showed that the Au(111)-(1×1) substrate was covered with a Ag bilayer as before the potential scan but with lower coverages of 0.84 and 0.37 ML for the first and second Ag layers, respectively.

This clearly shows that Ag atoms in the bilayer were partially stripped as a result of the reductive desorption of the C$_6$SH SAM.

The above results were summarized as follows:

1. When the Ag(2ML)/Au(111) was dipped in an ethanol solution containing 20 mM KOH and 0.1 mM C$_6$SH while keeping the potential at −1.4 V, the Ag UPD bilayer on the Au(111)-(1×1) surface perfectly remained on the Au(111)-(1×1) surface, as schematically shown in Fig. 3a.
2. When the potential of the Ag(2ML)/Au(111) was scanned in positive direction from −1.4 to 0 V in an ethanol solution containing 20 mM KOH and 0.1 mM C$_6$SH, C$_6$SH SAM was formed on the Ag(2ML)/Au(111) without pit formation, as schematically shown in Fig. 3b.
3. At −1.4 V after the potential was scanned to 0 V and then to −1.4 V, Ag atoms in the bilayer were partially

Table 1 Structure parameters at −1.4 V before the potential scan, at 0 V after the potential scan, and at −1.4 V after the potential cycle between −1.4 and 0 V obtained from the analyses of the reflectivity profiles at the Ag(2ML)/Au(111) electrode surface
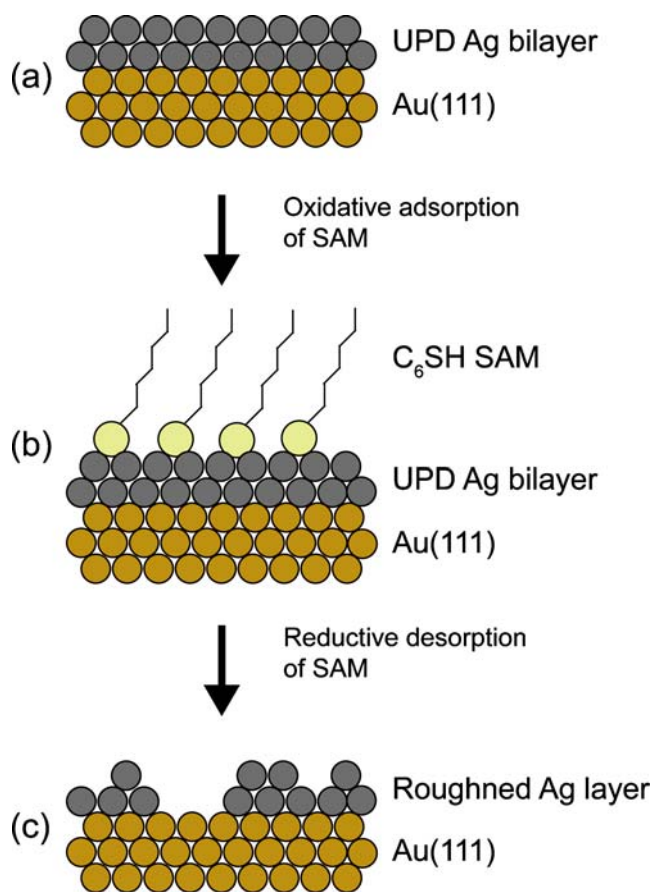
Distances[a]	−1.4 V (before the potential scan)	0 V (after the potential scan)	−1.4 V (after the potential cycle)
Distance, z_{Au-Au}	2.36±0.01	–	2.36±0.01
Distance, z_{Au-Ag}	2.35±0.01	2.36±0.03	2.36±0.02
Distance, z_{Ag-Ag}	2.36±0.02	2.36±0.03	2.36±0.02
Distance, z_{Ag-S}	–	2.82±0.13	–
Coverage, ρ_{Au}	1.00±0.01	–	1.00±0.01
Coverage, $\rho_{Ag(1)}$	0.99±0.03	1.00±0.01	0.84±0.06
Coverage, $\rho_{Ag(2)}$	0.99±0.02	0.99±0.02	0.37±0.05
Coverage, ρ_{S}	–	0.34±0.08	–
RMS, σ_{Au}	0.085±0.001	–	0.085±0.001
RMS, $\sigma_{Ag(1)}$	0.12±0.04	0.13±0.04	0.26±0.04
RMS, $\sigma_{Ag(2)}$	0.13±0.04	0.13±0.05	0.25±0.08
RMS, σ_{S}	–	1.21±0.16	–

[a] Distances of z_{Au-Au}, z_{Au-Ag}, z_{Ag-Ag}, and z_{Ag-S} represent atomic layer distances between the Au substrate and the top Au layer, between the Au substrate and the Ag layer, between two Ag layers, and between the Ag and S layers, respectively

Fig. 3 Schematic illustration of the interfacial structure of Ag(2ML)/Au(111) electrode in an ethanol solution containing 20 mM KOH and 0.1 mM C$_6$SH at **a** −1.4 V before the potential scan, **b** 0 V after the potential scan, and **c** −1.4 V after the potential cycle between −1.4 and 0 V

stripped as a result of the reductive desorption of the C_6SH SAM, as schematically shown in Fig. 3c.

These results show that one of the possible reasons for the vacancy island formation is an etching of silver surface atoms by alkylthiols, since SAM formation is usually carried out without potential control, and adsorption and desorption of the SAMs are taking place at the same time.

Conclusion

Surface structure of Ag bilayer with a (1×1) structure on Au(111) was not disturbed upon formation of a hexanethiol SAM in the alkaline ethanol solution but Ag atoms in the Ag bilayer were partially stripped as a result of the reductive desorption of the SAM, suggesting that the etching of the surface atoms is one of the important causes of the pit, i.e., vacancy island formation.

References

1. Ulman A (1991) An introduction to ultrathin organic films from Langmuir–Blodgett to self-assembly. Academic, New York
2. Ulman A (1996) Chem Rev 96:1533. doi:10.1021/cr9502357
3. Finklea HO (1996) In: Bard AJ, Rubinstein I (eds) Electroanalytical chemistry. vol. 19. Marcel Dekker, New York, p 109
4. Yamada R, Uosaki K (2008) In: Ariga K (ed) Bottom-up nanofabrication: supramolecules, self-assemblies, and organized films, Chap. 106. American Scientific, California (in press)
5. Kondo T, Uosaki K (2007) J Photochem Photobiol C Photochem Rev 8:1. doi:10.1016/j.jphotochemrev.2007.02.001
6. Uosaki K, Kondo T, Zhang X-Q, Yanagida M (1997) J Am Chem Soc 119:8367. doi:10.1021/ja970945p
7. Kondo T, Horiuchi S, Yagi I, Ye S, Uosaki K (1999) J Am Chem Soc 121:391. doi:10.1021/ja982007a
8. Kondo T, Kanai T, Uosaki K (2001) Langmuir 17:6317. doi:10.1021/la0108914
9. Poirier GE (1997) Chem Rev 97:1117. doi:10.1021/cr960074m
10. Edinger K, Gölzhäuser A, Demota K, Wöll C, Grunze M (1993) Langmuir 9:4. doi:10.1021/la00025a002
11. Schönenberger C, Sondag-Huethorst JAM, Jorritsma J, Fokkink LGJ (1994) Langmuir 10:611. doi:10.1021/la00015a001
12. Sondag-Huethorst JAM, Schönenberger C, Fokkink LGJ (1994) J Phys Chem 98:6826. doi:10.1021/j100078a027
13. Schönenberger C, Jorritsma J, Sondag-Huethorst JAM, Fokkink LGJ (1995) J Phys Chem 99:3259. doi:10.1021/j100010a042
14. Yamada R, Uosaki K (1997) Langmuir 13:5218. doi:10.1021/la970418j
15. Yamada R, Uosaki K (1998) Langmuir 14:855. doi:10.1021/la970974d
16. Yamada R, Wano H, Uosaki K (2000) Langmuir 16:5523. doi:10.1021/la991394e
17. Yamada R, Sakai H, Uosaki K (1999) Chem Lett 28:667. doi:10.1246/cl.1999.667
18. Wano H, Uosaki K (2005) Langmuir 21:4024. doi:10.1021/la050209w
19. Wano H, Uosaki K (2001) Langmuir 17:8224. doi:10.1021/la010990h
20. McDermott CA, McDermott MT, Green J-B, Porter MD (1995) J Phys Chem 99:13257. doi:10.1021/j100035a033
21. Bucher J-P, Santesson L, Kern K (1994) Langmuir 10:979. doi:10.1021/la00016a001
22. Dhirani A, Hines MA, Fisher AJ, Ismail O, Guyot-Sionnest P (1995) Langmuir 11:2609. doi:10.1021/la00007a046
23. Schweizer M, Kolb DM (2004) J Electroanal Chem 564:85. doi:10.1016/j.jelechem.2003.10.037
24. Hsieh M-H, Chem C (2000) Langmuir 16:1729. doi:10.1021/la990497u
25. Azzaroni O, Vela ME, Andreasen G, Carro P, Salvarezza RC (2002) J Phys Chem B 106:12267. doi:10.1021/jp0219653
26. Fonticelli M, Azzaroni O, Benítez G, Martins ME, Carro P, Salvarezza RC (2004) J Phys Chem B 108:1898. doi:10.1021/jp0359384
27. Kondo T, Morita J, Okamura M, Saito T, Uosaki K (2002) J Electroanal Chem 532:201. doi:10.1016/S0022-0728(02)00705-2
28. Ye S, Ishibashi C, Uosaki K (1999) Langmuir 15:807. doi:10.1021/la980812x
29. Kondo T, Morita J, Hanaoka K, Takakusagi S, Tamura K, Takahasi M, Mizuki J, Uosaki K (2007) J Phys Chem C 111:13197. doi:10.1021/jp072601j
30. Kondo T, Tamura K, Takahasi M, Mizuki J, Uosaki K (2002) Electrochim Acta 47:3075. doi:10.1016/S0013-4686(02)00226-8
31. Takahasi M, Hayashi Y, Mizuki J, Tamura K, Kondo T, Naohara H, Uosaki K (2000) Surf Sci 461:213. doi:10.1016/S0039-6028(00)00583-5
32. Widrig CA, Chung C, Porter MD (1991) J Electroanal Chem 310:335. doi:10.1016/0022-0728(91)85271-P
33. Kondo T, Sumi T, Uosaki K (2002) J Electroanal Chem 538/539:59. doi:10.1016/S0022-0728(02)01000-8
34. Sumi T, Wano H, Uosaki K (2003) J Electroanal Chem 550/551:321. doi:10.1016/S0022-0728(03)00141-4
35. Sumi T, Uosaki K (2004) J Phys Chem B 108:6422. doi:10.1021/jp049558+
36. Cometto FP, Paredes-Olivera P, Macagno VA, Patrito EM (2005) J Phys Chem B 109:21737. doi:10.1021/jp053273v
37. Yu M, Bovet N, Satterley CJ, Bengió S, Lovelock KRJ, Milligan PK, Jones RG, Woodruff DP, Dhanak V (2006) Phys Rev Lett 97:166102. doi:10.1103/PhysRevLett.97.166102